Catal Lett (2009) 129:71–78
DOI 10.1007/s10562-008-9794-9

Effect of Calcination Temperature of Kaolin Microspheres on the In situ Synthesis of ZSM-5

Hui Feng · Chunyi Li · Honghong Shan

Received: 23 June 2008 / Accepted: 20 November 2008 / Published online: 4 December 2008

Abstract ZSM-5 zeolite has been successfully synthesized in-situ on calcined kaolin microspheres by the hydrothermal method using n-butylamine as a template. The supported ZSM-5 was characterized by X-ray diffraction and scanning electron microscopy. The effect of calcination temperature of kaolin microspheres on the in-situ synthesis of ZSM-5 was investigated. The influence of the pretreatment temperature on the properties of kaolin microspheres including phase transformation, amounts of active SiO_2 and Al_2O_3, and pore structures, was studied using fourier transform infrared (FT-IR), nitrogen adsorption and chemical analysis. The results showed that when the calcination temperature increased from 300 to 900 °C, the amount of active SiO_2 in the kaolin microspheres increased slightly and the amount of active Al_2O_3 initially increased rapidly and then decreased steadily. The surface area and pore volume of the kaolin calcined at both low and high temperatures was less than those of kaolin calcined at a medium temperature. The property changes of kaolin caused the relative crystallinity of in situ synthesized ZSM-5 to vary.

Keywords Calcination temperature · Kaolin microspheres · In situ synthesis · ZSM-5

H. Feng · C. Li (✉) · H. Shan
State Key Laboratory of Heavy Oil Processing, China University of Petroleum, 257061 Dongying, China
e-mail: Chyli@hdpu.edu.cn

H. Shan
e-mail: Shanhh@hdpu.edu.cn

H. Feng
Chemical Engineering, University of Michigan, Ann Arbor, MI 48109, USA
e-mail: huifeng@umich.edu

1 Introduction

Propylene is an important industrial chemical; however, the supply is not keeping pace with its demand, as a result, research on increasing propylene production has become a topic of interest. ZSM-5 zeolite with three-dimensional sinusoidal and straight channels of molecular dimension was first used by Mobil in 1990s to increase the yield of propylene [1]. This zeolite selectively conducts cracking of C_7–C_{13} straight and short branched chain hydrocarbons to C_3–C_5 olefins. Thus, it enhances the octane of gasoline, increases the yield of light olefins and has become the preferred catalyst or additive for enhancing the yield of propylene in the field of petrochemical processing [2].

The method for in situ synthesis of ZSM-5 has significant advantages compared to the additive's traditional preparation. In the traditional method of preparation, the active component ZSM-5 is embedded in a binder or matrix which greatly reduces the contact between the feedstock and the active component. Consequently, the efficiency of ZSM-5 zeolite is decreased. Using the method of in situ synthesis, ZSM-5 zeolite can be synthesized on the surfaces of kaolin microspheres, thus allowing the feed oil easy access to the active component. Furthermore, if the shape of microspheres is preserved, the composite materials can be directly used as an additive.

At present, only a few research papers on in situ synthesis of ZSM-5 additive are available [3–9]. However, there are more reports about in situ synthesis of cracking catalyst containing Y zeolite. Walter et al. [10] reported that the kaolin which was calcined at 982 °C can be activated to sources of silica and alumina for the synthesis of zeolite X or zeolite Y. Dight et al. [11] showed that chemically active SiO_2 and Al_2O_3 in the preformed

calcined kaolin were the "nutrients" used during the synthesis of molecular sieves. Zheng et al. [12] investigated the association between calcination temperature and active SiO_2 and Al_2O_3 in the range of 750–1,200 °C. In this paper, the active SiO_2 that they reported is amorphous silicon dioxide, while the active Al_2O_3 is tetrahedral Al. In the process of in situ synthesis, all or part of the active SiO_2 and Al_2O_3 were used to synthesize molecular sieves within the channels of preformed kaolin microspheres. Thus, the calcination temperature of kaolin microspheres is a very influential factor in determining the amounts of active SiO_2 and Al_2O_3 for the synthesis of zeolite. Reports available in the literature about in situ synthesis of ZSM-5 [3–9] only described calcination of kaolin microspheres at 1,000 °C or higher, but no low temperature studies have been undertaken, and more important, lower calcination temperatures should make the ZSM-5 catalyst less expensive to produce.

In the previous experiments performed in our laboratories, ZSM-5 has been synthesized successfully in situ on kaolin microspheres calcined at 700 °C. And we have systematically investigated the effects on synthesis variables on the synthesis of ZSM-5 zeolite, including SiO_2 to Al_2O_3 ratio, pH, crystallization time, and crystallization temperature [13]. However, it is necessary to carry out further detailed investigations of the in situ synthesis of ZSM-5 within the broad low calcination temperature range and to get better understanding how the calcination temperature of kaolin affected the synthesis of ZSM-5.

The objective of this paper is to study the effect of the calcination temperature on the relative crystallinity of synthesized ZSM-5 zeolite in the temperature range between 300 and 900 °C. Insights gained will contribute to the development of kaolin- supported catalysts for the Fluid Catalytic Cracking (FCC) reaction.

2 Experimental Procedures

2.1 Raw Materials

Kaolin was provided by China Kaolin Clay Company. Silica sol (40wt% SiO_2, industrial grade) was supplied by a chemical factory of Qingdao, China. Water glass (34wt% solid, SiO_2/Na_2O (mol/mol) = 3.3, industrial grade) was obtained from the catalyst factory of Zhoucun, China. Butylamine (chemical grade) and sodium nitrate (analytical grade) were purchased from the China Medicine Group Chemical Regent Co. Ltd. The chemical composition of kaolin was determined by the ICP method and is given in Table 1. Mineral structural analysis of the kaolin sample was carried out by the XRD, and the XRD pattern of the kaolin sample (JCPDS 01-078-1996) is given in Fig. 1.

Table 1 Chemical analysis of Kaolin mineral

Component	Wt%
SiO_2	46.19
Al_2O_3	37.80
TiO_2	0.52
Fe_2O_3	0.35
CaO	0.08
MgO	0.05
Na_2O	0.62
K_2O	0.63
LOI	13.76

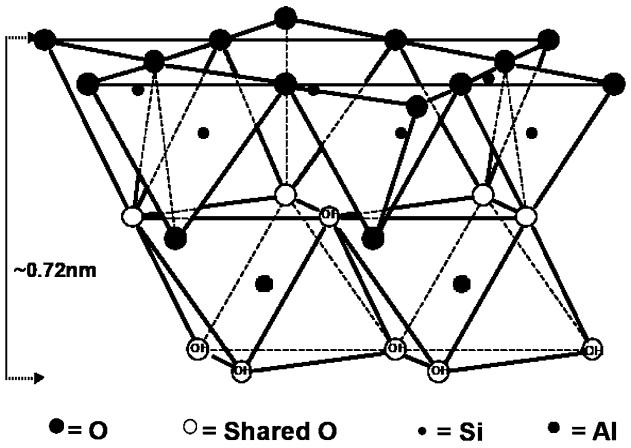

Fig. 1 Schematic diagram of Kaolin structure

2.2 Hydrothermal Synthesis

Kaolin was added under constant stirring to the silica sol to form a 1:2 weight ratio of kaolin to silica. After stirring for 2 h, the blend was dried at 160 °C. The dry mixture was then calcined at different temperatures for 2 h in a muffle furnace, followed by grinding and screening into microparticles with a diameter of 88–188 μm. This mixture is referred to as calcined kaolin microspheres (CKM).

The synthesis of ZSM-5 was carried out by combining CKM, water glass, *n*-butylamine, sodium nitrate and distilled water, giving the following molar oxide ratio: $0.20Na_2O{:}1.00SiO_2{:}0.01Al_2O_3{:}0.08C_4H_{11}N{:}15.00H_2O$. The final pH of the mixture was adjusted by a hydrochloric acid (HCl) addition. After stirring for 2 h at room temperature, the mixture was placed in a 35 ml stainless steel autoclave. After reacting for 72 h at 160 °C, a solid cake was recovered from the slurry through filtration, and then washed several times with distilled water. A crystalline product was obtained by drying the solid cake at 120 °C in air atmosphere for 2 h.

2.3 Characterization of Crystallized Products and CKM

XRD was performed using the X'Pert PRO MPD (DANalytical Co.) diffractometer with Cu-Kα radiation (45 kV, 40 mA). The sum of peak intensities at 2θ of 7.9°, 8.7°, 23.0°, and 23.9° for the experimental ZSM-5 zeolite (JCPDS 00-039-0225) was compared to the sum of peak intensities for the commercial ZSM-5 zeolite. Commercial ZSM-5 zeolite was provided by Nankai University, China. This ratio of the experimental ZSM-5 to the commercial ZSM-5 is referred to as the relative crystallinity. The amount of zeolite mordenite (MOR) (JCPDS 00-049-0924) formed during crystallization was estimated by the sum of peak intensities at 2θ of 9.8°, 13.5°, 19.7°, 22.3°, 25.7°, 26.3°, and 27.7°, while the sum of peak intensities at 2θ of 12.5°, 17.7°, 21.7°, 28.2°, and 33.5° represented the amount of the impurity NaP zeolite (JCPDS 00-040-1464).

SEM images of products were acquired on a QUANTA 200 3D. The specific surface area and pore volume of the CKM were determined by N_2 adsorption on a Micromeritics ASAP2010 at −196 °C. The pore size distribution was calculated from the desorption branches of the isotherms using BJH methods. The micropore volume and micropore surface area were calculated using a t-plot.

The IR vibrational signature of the CKM was determined using a Nexus Model Infrared Spectrophotometer (Thermo Nicolet). The FT-IR spectrum of the CKM was recorded in the range 4,000–400 cm^{-1} in wafers of KBr mixed with 1% (w/w) of sample. Thermo gravimetric (TG) and differential thermal analyses (DTA) were recorded on a Beijing Optics Instrument Ltd. WCT-2 at a heating rate of 10 °C/min, in air atmosphere.

Active SiO_2 can be expressed by alkali solubility. The calcined microspheres were soaked in 24% NaOH at 90 °C for 1 h, and then filtered, and the SiO_2 amount in the liquid was analyzed by the potassium silicofluoride volumetric analysis. Active Al_2O_3 can be characterized by acid solubility. The experimental procedure was done according to the patent [11].

3 Results and Discussion

3.1 Phase Transformation Behavior of Kaolin

Kaolin is a clay mineral with the chemical composition $Al_2Si_2O_5(OH)_4$. Its structure, as illustrated in Fig. 2, is composed of an octahedral alumina layer joined to a tetrahedral silica layer via shared apical oxygen. The heat treatment of kaolin transforms them into metakaolin, and higher temperature treatment leads to mullite and critobalite [14]. It is useful to discuss the calcination chemistry of kaolin from the point of view of its importance in the conversion process from kaolin to zeolite.

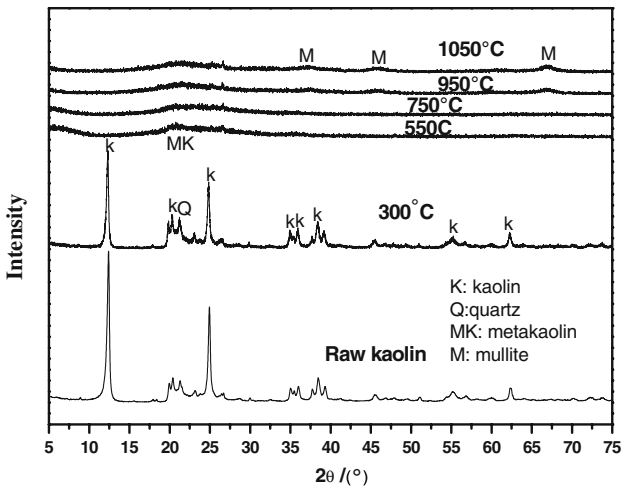

Fig. 2 XRD patterns of kaolin and CKM calcined at different temperatures

The DTA curves of the kaolin sample (Fig. 3) show strong endothermic peaks at 539 °C, due to dehydroxylation, and at 1,002 °C, due to the formation of new solid phase. These results are in agreement with XRD results. In Fig. 1, at 550 °C the amorphous peaks of metakaolin appeared instead of kaolin specific peaks, which indicate the first step of the transformation process. Kaolin was transformed to the metakaolin phase with a loss of structural hydroxyl groups during the occurrence of an endotherm as noted in DTA. At 950–1,050 °C mullite specific peaks appeared which indicate that in the second step the metakaolin decomposes and forms a mullite phase. Therefore, the thermal behavior of Sunzhou kaolin is similar to other kaolin described in the literature [15]. At the range of 300–900 °C, there is only one phase transformation.

3.2 Effect of Calcination Temperature on the Properties of Kaolin Microphores

3.2.1 Active Al_2O_3 and Active SiO_2[1] in the CKM

Figure 4 presents the IR spectra of kaolin microspheres which were calcined at different temperatures. Assignments of the IR vibration frequencies for the experimental and literature data of kaolin are given in Table 2. The main IR functional bands of CKM were similar to those IR characteristics for raw kaolin [16] when the temperature was 300 °C. With an increasing calcination temperature, an increase for the absorbance in the 810 cm^{-1} region, and a decrease in the regions of 540, 912 and 3,620–3,690 cm^{-1}

[1] Active SiO_2 in CKM originated from kaolin and silica binder.

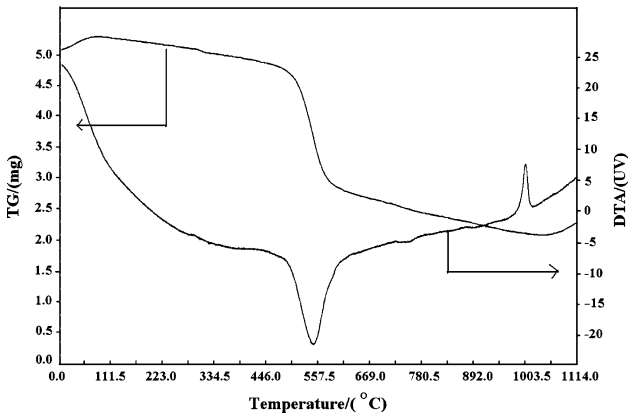

Fig. 3 DTA/TG curve of Kaolin

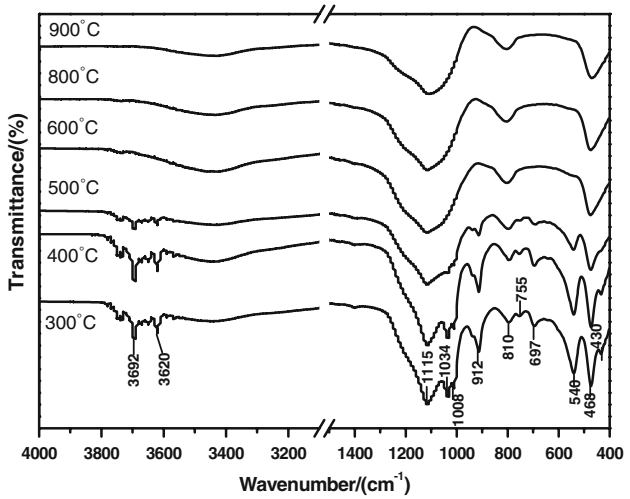

Fig. 4 FT-IR spectra of CKM calcined at different temperatures

were observed. These data show that at calcination temperatures less than 500 °C, the absorbed water, free water and hydrogen-bonded water in the CKM can be released [19]. The number of hexa-coordinated Al decreases gradually as it converts to much more reactive tetra- and penta-coordinate Al [17, 18]. When the calcination temperature reached 600 °C, the absorbance in the 3,620–3,690, 912, and 540 cm^{-1} region disappeared. There were only several peaks at 1,071, 810, and 468 cm^{-1}, which are the characteristic bands of metakaolin [15]. This indicates that the kaolin transforms to the metakaolin phase at 600 °C, which is in accordance with the results of DTA and XRD measurements. With a further increase of temperature, the vibration band of AlO4 tetrahedron in the IR remains nearly constant, but decreases slightly after 800 °C. This demonstrates that the number of chemically active tetra- or penta-coordinate Al is reduced. There was no significant change in the 468 cm^{-1} region assigned to T–O (SiO4) deforming vibrations, which suggests that calcination temperature has little effect on the SiO4 tetrahedron.

The amounts of active SiO_2 and Al_2O_3 of CKM calcined at different temperatures are shown in Fig. 5. This active SiO_2 increased from 22 to 26%, which changed slightly further confirming that dehydroxylation had little effect on the SiO_4 tetrahedron. While, active Al_2O_3 first increased and then decreased. The curve is steep over the range of 300–600 °C, indicating that the number of active aluminum sites increases significantly and more hexa-coordinated aluminums convert to tetra- and penta-coordinate aluminums. When the calcination temperature was increased to 700 °C, the numbers of active aluminum sites reached a maximum. After 700 °C, the number decreased slowly. These results coincide with the FT-IR analysis. A similar observation was made by Zheng et al. [12] who found that in the range of 750–900 °C the amount of active SiO_2 in the CKM increased while the amount of active Al_2O_3 decreased.

3.2.2 *Pore Structure of CKM*

The N_2 adsorption–desorption isotherms of raw kaolin and CKM at different calcination temperatures are presented in Fig. 6. The adsorption–desorption isotherms for the CKM [Fig. 6(2–5)] were typical of Type IV sorption isotherms which show obvious hysteresis loops for the H-2 type. H-2 type is broad with the desorption branch being much steeper than the adsorption branch and is encountered within the relative pressure p/p_0 ranging from 0.5 to 1.0, suggesting that the distribution of pore sizes and pore shapes is broad. A sudden change in the adsorption branch curve resulting from capillary condensation was observed

Table 2 IR vibrational frequencies of the experimental and literature data of kaolinite

Vibrations	Wave number (cm^{-1}) (experimental)	Literature wave number (cm^{-1}) [17, 28–31]
υ(OH)	3,620,3,696	3,620,3,695
δ(OH)	912	912
υ(SiO)	1,115,1,008	1,116,1,010
AlO4 stretching	810	810
$Al(O,OH)_6$ stretching	540	540
Si–O deformation	468,430	469,428

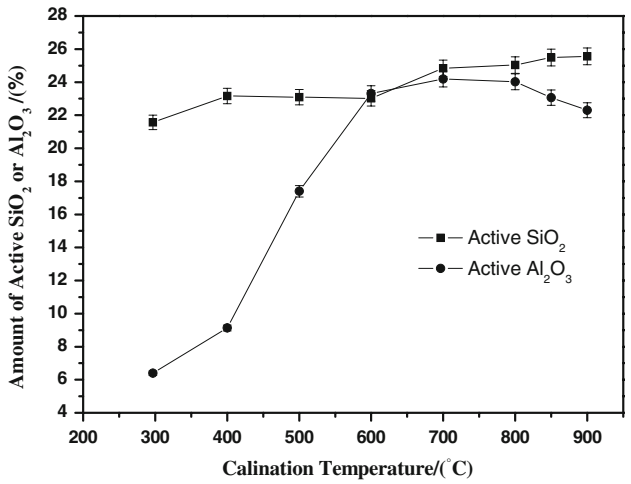

Fig. 5 The amount of active SiO_2 or Al_2O_3 in CKM calcined at different temperature

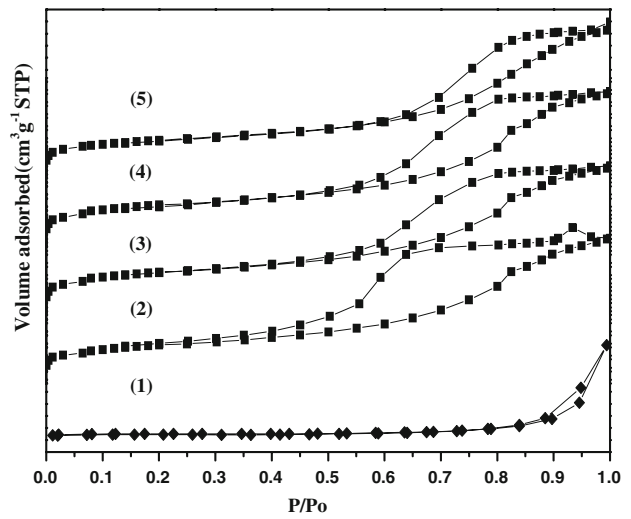

Fig. 6 Adsorption–desorption isotherms (nitrogen) of kaolin and CKM calcined at different temperature (*1*) raw kaolin (*2*) 300 °C, (*3*) 500 °C, (*4*) 700 °C, (*5*) 850 °C

in the Type IV sorption isotherms. It is reported that the higher the pressure causing capillary condensation, the larger the pore size of the sample [20]. Therefore, the pore size of CKM increased with an increase of the calcination temperature. However, the isotherm of the raw kaolin was different [Fig. 6(1)]. The isothermal was typical of Type III sorption isotherms with hysteresis loops of the H-3 type, and which do not exhibit any limiting adsorption at high p/p_0. It is believed that this type of isotherm occurs with aggregates of plate-like particles giving rise to slit-shaped pores [21]. The pore size is in the range of large pores.

The pore structure parameters of the raw kaolin and CKM at different calcination temperatures are summarized in Table 3. In the process of in situ synthesis, zeolites are synthesized on accessible surfaces of kaolin microspheres' channels [22]. The larger the specific surface area and pore volume are, the more is beneficial to the synthesis of zeolite. Interestingly, there are many large pores in the raw kaolin, but the specific surface areas and pore volumes of raw kaolin are very small. Compared with raw kaolin, the specific surface areas and pore volumes of CKM clearly increased and small amounts of micropores appeared. The specific surface area and pore volume of CKM calcined at low or high temperatures was lower than those of CKM calcined at a medium temperature. Therefore, the kaolin microspheres calcined at a medium temperature favored zeolite synthesis.

3.3 Effect of Calcination Temperature of CKM on the Synthesis of ZSM-5

The XRD patterns of products synthesized on CKM calcined at different temperatures are shown in Fig. 7. The peaks in the XRD patterns of products can be indexed from the American Society for Testing and Materials (ASTM) data. The XRD pattern shows peaks at ranges of $2\theta = 7$–$9°$ and 23–25°, which correspond well to the specific peaks of ZSM-5 zeolite. This indicates that the products obtained contain ZSM-5 crystals. Figure 8 presents the scanning electron microscope photographs of CKM and in situ synthesized products at different crystallization time. The shapes of CKM are irregular because they are made by grinding and screening rather than by spray drying. Compared to the picture of CKM in Fig. 8(1), a zeolite crystal

Table 3 Effect of calcination temperature on surface area and pore volume of CKM

Sample	Calcination temperature (°C)	Total surface area ($m^2\ g^{-1}$)	Micropore surface area ($m^2\ g^{-1}$)	Total pore volume ($cm^3\ g^{-1}$)	Micropore pore volume ($cm^3\ g^{-1}$)
S[a]	–	15.1	0.0	0.008	0.000
S3	300	82.7	1.3	0.170	0.000
S5	500	94.0	6.9	0.173	0.003
S7	700	91.2	5.9	0.181	0.002
S8	850	77.2	3.5	0.171	0.001

[a] Raw kaolin

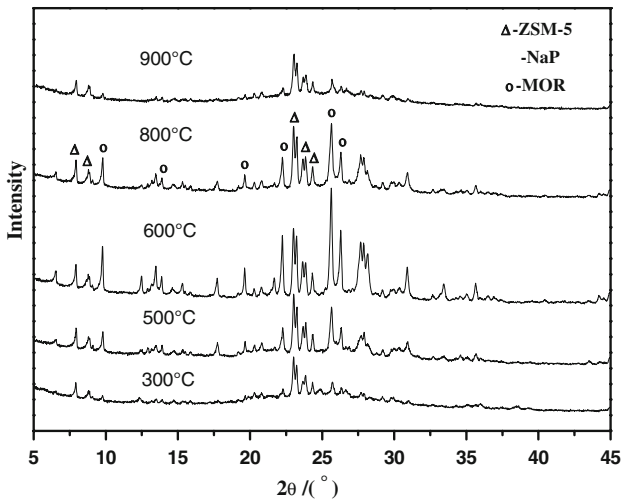

Fig. 7 XRD patterns of synthesized products on CKM calcined at different temperature

layer was formed on the outer surface of the synthesized product [Fig. 8(2, 3)]. With the magnified SEM picture [Fig. 8(4)], we can see clearly that the morphology of synthesized zeolite ZSM-5 is cuboidal, which is the typical crystal shape of ZSM-5 when using n-butylamine as a structure-directing agent [23]. The crystal size is about 10 μm, which is approximately twice as large as is most often reported for ZSM-5 crystals. The amount of ZSM-5 on the CKM was changed as the crystallization time changed. While the crystallization time was 36 h, the amount of ZSM-5 was so little that the kaolin microsphere was not covered completely. With an increase of crystallization time to 72 h, the kaolin microsphere was covered completely.

Figure 9 presents the changes of relative crystallinity of ZSM-5 over different calcination temperatures. The crystallinity of ZSM-5 synthesized on CKM calcined at a medium temperature of 600–800 °C was higher than that of ZSM-5 synthesized on CKM calcined at 300–600 °C or 800–900 °C. During in situ synthesis, as the crystallization reaction proceeds, some of the silica in the kaolin microspheres is dissolved into the solution by alkali leaching, which forms some channels in the microspheres. The zeolite crystals can grow on the inner surfaces of microspheres [24]. Based on the results above, when the calcination temperature exceeded 500 °C, kaolin was transformed into metakaolin and the tetrahedral sheet was broken, which further increased the degree of disorder and made the amount of soluble silica species increase rapidly [25]. The increase of soluble silica promoted the fast polymerization of aluminosilicate species in the solution

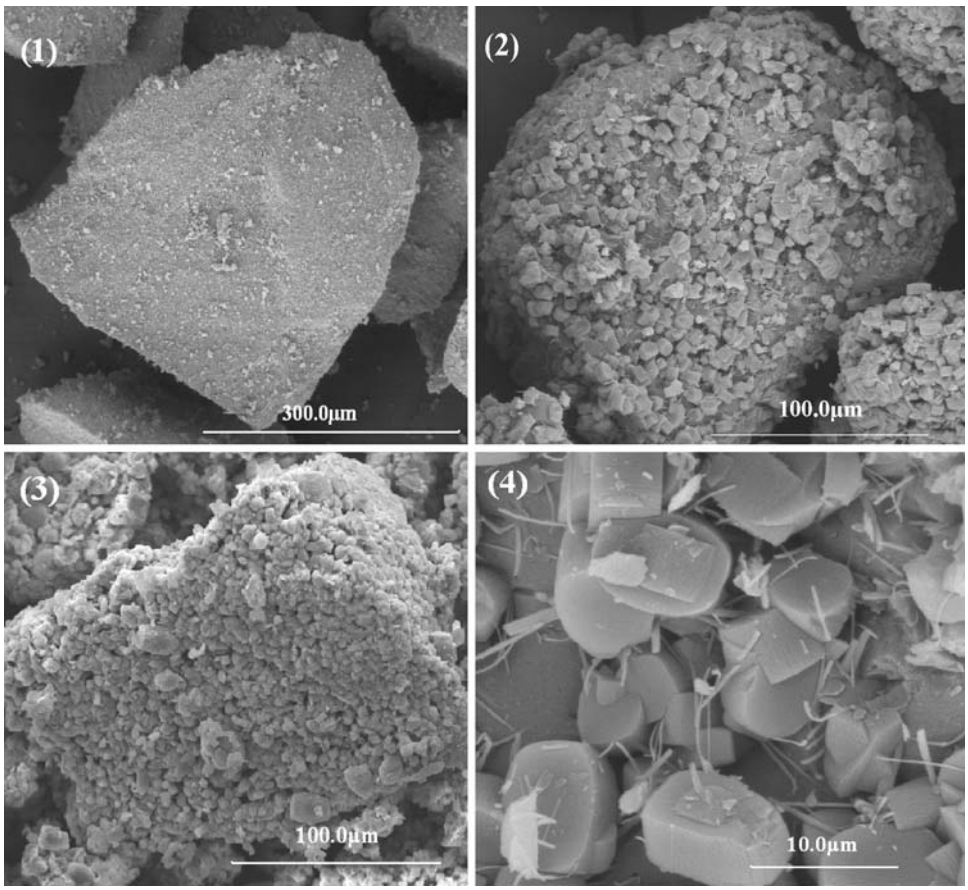

Fig. 8 SEM photographs of CKM calcined at 700 °C (**a**) and products obtained for 36 h (**b**) 72 h (**c**) 36 h (**d**)

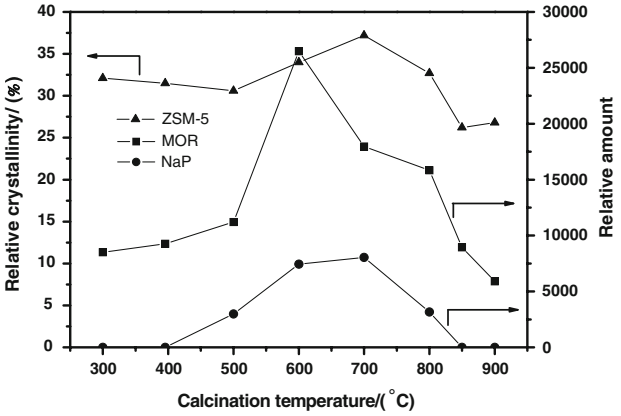

Fig. 9 Effect of calcination temperature on the relative crystallinty or amount of synthesized products

and gel formation and it further induced nucleus formation. Finally, the combined results of these procedures accelerate the growth of the zeolite. Therefore, the crystallinity of ZSM-5 increased with calcination temperature increasing from 500 to 600 °C. As the calcination temperature was further increased, heating at 800 °C produced complete dehydroxylation [25]. Thus, the crystallinity of ZSM-5 was higher when the temperature was higher than 500 °C. However, after 800 °C, one of the probable reasons for the decrease of ZSM-5 crystallinity is the decrease of the specific surface area of kaolin microspheres.

From Fig. 7, the characteristic peaks of MOR and GIS structures appeared, which indicated that there was MOR and NaP zeolite impurity in addition to ZSM-5 zeolite. The crystallization conditions of MOR and ZSM-5 are similar, so it is not surprising that mixed crystals are formed [26]. Although the NaP zeolite appears frequently in the process of in situ synthesis of Y zeolite [27], it seldom appears in the process of in situ synthesis of ZSM-5 zeolite. In Fig. 9, the amounts of MOR and NaP zeolites were also influenced by the calcination temperatures. The amounts of the two zeolites first increased and then decreased with increasing temperatures. Both MOR and NaP zeolites appeared together in the medium temperature range of 500–800 °C, in which the kaolin transforms into metakaolin. However, the NaP did not form in the high or low temperature range. In the mid-temperature range, due to dehydroxylation, kaolin presents the lowest stability against an NaOH attack which produces a fast increase of the amount of $Al(OH)_{4-}$ and SiO_4^{4-} species in solution [25]. From the FT-IR and acid solubility analysis, hydroxylation has the greatest effect on the $Al(O,OH)_6$ octahedron sheets. The octahedron sheets convert to tetrahedron sheets which causes more hexa-coordinated Al transform into reactive tetra- and penta-coordinated Al. SiO_4^{4-} species and Al $(OH)_{4-}$ species are then polymerized to form an initial aluminosilicate gel of a lower silica–alumina ratio. However, under the same crystallization conditions, the silica–alumina ratio of the initial aluminosilicate gel for the formation of zeolite MOR is lower than that of the initial aluminosilicate gel for the formation of zeolite ZSM-5. While, the silica–alumina ratio of the initial aluminosilicate gel for the formation of zeolite NaP is the lowest. Therefore, the initial Al-rich gel phase favored MOR and NaP zeolite formation. Also, in the mid-temperature range, the kaolin microspheres have larger specific surfaces and pore volumes, which may be one of the favorable conditions for the formation of zeolite MOR and NaP.

4 Conclusions

ZSM-5 zeolite was successfully synthesized in situ on kaolin microspheres calcined in the range of 300–900 °C. The morphology of the zeolite was determined to be cuboidal and about 10 μm in length.

When the calcination temperature increased from 300 to 900 °C, the amount of active SiO_2 in the CKM increased slightly and the amount of active Al_2O_3 initially increased rapidly and then decreased steadily. The surface area and pore volume of the kaolin microspheres calcined at the medium temperature range was higher than those of CKM calcined at a low or high temperature ranges.

The relative crystallinity of ZSM-5 was higher when the kaolin microsphere was calcined at the medium temperature range of 600–800 °C, and lower when the kaolin microspheres was calcined at the low temperature range of 300–500 °C or high temperature range of 800–900 °C. Using the kaolin microspheres calcined at the low or high temperature ranges as the raw material, the amount of associated phase MOR or NaP could be decreased.

Acknowledgments Financial support was provided by Petrochina Company under cooperative agreement 040806-01-00. The authors thank the Instrument Anaylisi Center at China University of Petroleum for the XRD, BET and FT-IR analysis.

References

1. Degnan TF, Chitnis GK, Schipper PH (2000) Microporous Mesoporous Mater 35–36:245
2. Abul-Hamayel MA, Aitani AM, Saeed MR (2005) Chem Eng Technol 28:923
3. Dwyer FG, Schwartz AB (1978) US patent 4091007
4. Chu P, Pasquale GM (1985) US patent 4522705
5. Rosinski EJ, Chu P, West AH (1985) EP 0156595A2
6. McWilliams JP, Woodbury NJ (1992) US patent 5145659
7. Xu M, Macaoay J (2005) US patent 0181933
8. Sun SH, Ma JT, Pang XM, Gao XH, Song MF (2006) J Chin Ceram Soc 34:757
9. Sun SH, Ma JT, Gao XH (2007) Clay Miner 42:203

10. Haden WL Jr, Dzierzanowski FJ (1972) US patent 3663165
11. Dight LB, Leskowicz MA, Bogert DC (1989) EP 0369629
12. Zheng SQ, Chang XP, Gao XH (2002) Non-Met Mines 25:5
13. Feng H, Li CY, Shan HH, Appl Clay Sci. doi:10.1016/j.clay.2008.05.004
14. Rocha J, Klinowski J (1990) J Angew Chem 102:539
15. Kakali G, Perraki T, Tsivilis S, Badogiannis E (2001) Appl Clay Sci 20:73
16. Alkan M, Hopa C, Yilmaz Z, Guler H (2005) Microporous Mesoporous Mater 86:176
17. Lambert JF, Millman WS, Fripiat JJ (1989) J Am Chem Soc 111:3517
18. Akolekar D, Chaffee A, Howe RF (1997) Zeolite 19:359
19. Chen GH, Liang HD (2005) J Foushan Ceram 107:9
20. Xu RR, Pang WQ, Yu JH, Huo QS, Chen JS (2004) Molecular sieves and porous materials chemistry. Science Press, Beijing
21. Rouquerol F, Rouquerol J, Sing K (1999) Adsorption by powdors and porous solids principles, methodology and applications. Academic Press, San Diego
22. Zheng SQ, Wang ZF, Tan ZG, Gao XH, Xu XL (2006) Pet Technol & App 24:104
23. Sang SY, Chang FX, Liu ZM, He CQ, He YL, Xu L (2004) Catal Today 93–94:729
24. Shen JH, Mao XW, Yuan SL, Zhang YM (1996) Acta Petrolei Sin (Pet Process Sec) 12:20
25. Madani A, Aznar A, Sanz J, Serratosa JM (1990) J Phys Chem 94:760
26. Ma ZL, Zhao TB, Zong BN (2004) Acta Petrolei Sin (Pet Process Sec) 20:21
27. Chandrasekhar S, Pramada PN (2004) Appl Clay Sci 27:187
28. Markovic S, Dondur V, Dimitrijevic R (2003) J Mol Struct 654:223
29. Johnston CT, Bish DL, Eckert J, Brown L (2000) J Phys Chem B 104:8080
30. Yariv S, Lapides I, Michaelian KH, Lahav N (1999) J Them Anal Calorim 56:865
31. Saikia NJ, Bharali DJ, Sengupta P, Bordoloi D, Goswamee RL, Saikia PC, Borthakur PC (2003) Appl Clay Sci 24:93